An all-optical buffer based on polarization rotation in an EAM*

Wang Kui-Ru(王葵如)†, Kuang Hai(匡 海), Wang Yong-Jun(王拥军),
Yuan Jin-Hui(苑金辉), and Yan Bin-Bin(颜玢玢)

State Key Laboratory of Information Photonics and Optical Communications, Beijing University of Posts and Telecommunications, P. O. Box 72, Beijing 100876, China

(Received 6 January 2013; revised manuscript received 6 February 2013)

A theoretical model of the refractive index changes of the TE and TM modes in an electro-absorption modulator (EAM) is deduced. The photon absorption and refractive index changes are analyzed numerically. The influence of pump intensity on the phase difference between the TE and TM modes is studied. The polarization rotation effect is obtained in the EAM, and a novel all-optical fiber loop buffer is designed.

Keywords: electro-absorption modulator, polarization rotation effect, all-optical fiber loop buffer

PACS: 42.25.Ja, 42.25.Lc, 42.79.–e **DOI:** 10.1088/1674-1056/22/8/084201

1. Introduction

The all-optical buffer is the key component of an all-optical switching network. A review of previous studies reveals that the all-optical buffer-based fiber ring is most practical.[1] Based on the Franz–Keldysh effect,[2] an electro-absorption modulator (EAM) is an optical signal modulator which has the advantages of low power, fast processing, and a simple process. Meanwhile, it can achieve both electro–optic operation and optic–optic operation. It is already widely used in high-speed communication systems for coded modulation,[3] ultrashort pulse generation,[4] and wavelength conversion.[5] Also, it can be integrated with other devices to accomplish even more functions.[6–8]

However, the polarization property of EAMs is often ignored. In recent years, it is well known that an EAM can cause a significant change in refractive index[9] when the change in the carrier concentration reaches 10^{18} cm^{-3}. For the TE and TM modes of input light, the changes of the refractive index values are not exactly equal, which leads to a phase difference between them. In Refs. [10] and [11], the wavelength conversion is achieved by controlling the specific polarization of the output light, but no theoretical model of the refractive index difference was given.

In this paper, a theoretical model of the refractive index changes both parallel and perpendicular to the waveguide surface in the situation of strong light injection into the EAM is deduced. And the influence of light intensity and photon-generated carrier concentration on the refractive index difference between the TE mode and TM mode is analyzed. Finally, a novel fiber ring all-optical buffer is designed based on polarization rotation switching of an EAM. Compared with a similar all-optical buffer-based semiconductor optical amplifier (SOA), this all-optical buffer has a faster read-write speed.

2. Theoretical model

If a beam of continuous light is injected into a rectangular waveguide of a semiconductor, the photon-generated carrier concentration in the stable state can be described as[12]

$$\Delta N = \sqrt{I_0 \alpha \beta \left(1 - R\right) \mathrm{e}^{-\alpha z} / h\upsilon B_{\mathrm{r}}}, \tag{1}$$

where I_0 is light intensity, α is the absorption coefficient of the semiconductor material for the pump light, β is the quantum efficiency, R is the reflection coefficient of the interface between air and the semiconductor, z is the distance along the direction of the pumping light irradiation, h is Planck's constant, υ is the pump light frequency, and B_{r} is the radiation recombination coefficient. Equation (1) shows the stable-state carrier distribution in stable uniform illumination along the beam direction. Photon-generated carrier concentration is proportional to the square root of the pump light intensity.

When a beam of signal light is launched into the waveguide (Fig. 1), the change of the carrier concentration induced by the pump light leads to different absorption coefficients for the TE and TM modes of the signal light. According to the Kramers–Kronig constraint, the changes in the refractive indices of the TE and TM modes are not equal.

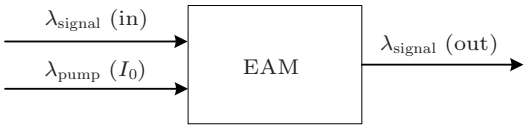


Fig. 1. Schematic diagram of input/output in rectangular waveguide

In the long-wavelength range, the free-carrier absorption and band filling effect are the primary factors to bring

*Project supported by the National Natural Science Foundation of China (Grant No. 61077014) and the National Basic Research Program of China (Grant No. 2010CB327601).

†Corresponding author. E-mail: krwang@bupt.edu.cn

© 2013 Chinese Physical Society and IOP Publishing Ltd

about a variation of absorption coefficient along with a change of photon-generated carrier concentration. Because the free-carrier absorption has the same effect on both the TE and TM modes, only the band filling effect is considered here.

In the band filling effect, the changes of the absorption coefficients along with the carrier concentration are given by the square root law[13]

$$\Delta\alpha(N,P,E) = \frac{C_{\rm hh}}{\upsilon}\sqrt{\upsilon-\upsilon_{\rm g}}\left[f_v\left(E_{\rm ah}\right)-f_{\rm c}\left(E_{\rm bh}\right)-1\right] + \frac{C_{\rm lh}}{\upsilon}\sqrt{\upsilon-\upsilon_{\rm g}}\left[f_v\left(E_{\rm al}\right)-f_{\rm c}\left(E_{\rm bl}\right)-1\right], \quad (2)$$

where N and P are the concentrations of free electrons and holes, E is photon energy ($E = h\upsilon$), $E_{\rm g}$ represents band-gap energy for the material, C is a constant, $\upsilon_{\rm g} = E_{\rm g}/h$, $f_{\rm c}\left(E_{\rm b}\right)$ is the probability of a conduction band state of energy $E_{\rm b}$ occupied by an electron, $f_v\left(E_{\rm a}\right)$ is the probability of a valence band state of energy $E_{\rm a}$ occupied by an electron, and $E_{\rm b}$ and $E_{\rm a}$ denote energy in the conduction band and valence band respectively.[13]

The probabilities $f_{\rm c}$ and f_v are given by the Fermi-Dirac distribution functions

$$f_{\rm c}\left(E_{\rm bh,bl}\right) = \left[1+{\rm e}^{\left(E_{\rm bh,bl}-E_{\rm Fc}\right)/\left(k_{\rm B}T\right)}\right]^{-1}, \quad (3)$$

$$f_{\rm v}\left(E_{\rm ah,al}\right) = \left[1+{\rm e}^{\left(E_{\rm ah,al}-E_{\rm Fv}\right)/\left(k_{\rm B}T\right)}\right]^{-1}, \quad (4)$$

where $k_{\rm B}$ is Boltzmann's constant, and T is absolute temperature. $E_{\rm F_c}$ and $E_{\rm F_v}$ are the carrier-dependent quasi-Fermi levels. They can be estimated by the Nilsson approximation[14]

$$E_{\rm F_c} = \left\{\ln\left(\frac{N}{N_{\rm c}}\right)+\frac{N}{N_{\rm c}}\left[64+0.05524\frac{N}{N_{\rm c}} \times\left(64+\sqrt{\frac{N}{N_{\rm c}}}\right)\right]^{-(1/4)}\right\}k_{\rm B}T, \quad (5)$$

$$E_{\rm F_v} = \left(-\left\{\ln\left(\frac{P}{N_{\rm v}}\right)+\frac{P}{N_{\rm v}}\left[64+0.05524\frac{P}{N_{\rm v}} \times\left(64+\sqrt{\frac{P}{N_{\rm v}}}\right)\right]^{-(1/4)}\right\}-E_{\rm g}\right)k_{\rm B}T. \quad (6)$$

Applying energy and momentum conservation, equation (7) can be written as

$$E_{\rm ah,al} = \left(E_{\rm g}-E\right)\left(\frac{m_e}{m_e+m_{\rm hh,lh}}\right)-E_{\rm g}, \quad (7)$$

$$E_{\rm bh,bl} = \left(E-E_{\rm g}\right)\left(\frac{m_{\rm hh,lh}}{m_e+m_{\rm hh,lh}}\right), \quad (8)$$

where $m_{\rm e}$, $m_{\rm hh}$, and $m_{\rm lh}$ refer to the effective masses of electrons, heavy holes, and light holes, respectively.

It can be seen on the right-hand side of Eq. (2) that the first term refers to the impact of heavy holes, and the second term is related to the light holes. In addition, the absorption activities of the TE and TM modes separately generate heavy holes and light holes. Therefore, equation (2) can be rewritten into the forms

$$\Delta\alpha\left(N,P,E\right) = \Delta\alpha_{\rm TE}+\Delta\alpha_{\rm TM}, \quad (9)$$

$$\Delta\alpha_{\rm TE} = \frac{C_{\rm hh}}{\upsilon}\sqrt{\upsilon-\upsilon_{\rm g}}\left[f_v\left(E_{\rm ah}\right)-f_{\rm c}\left(E_{\rm bh}\right)-1\right], \quad (10)$$

$$\Delta\alpha_{\rm TM} = \frac{C_{\rm lh}}{\upsilon}\sqrt{\upsilon-\upsilon_{\rm g}}\left[f_v\left(E_{\rm al}\right)-f_{\rm c}\left(E_{\rm bl}\right)-1\right]. \quad (11)$$

According to the Kramers–Kronig constraint, the change in refractive index is given by

$$\Delta n\left(N,P,E\right) = \frac{hc}{\pi e}\int_0^\infty \frac{\Delta\alpha\left(N,P,E'\right)}{E'^2-E^2}{\rm d}E'. \quad (12)$$

Without illumination there is so little free-carrier concentration that it has almost no effect on the changes of refractive indices. With high illumination, the photon-generated carrier concentration is far higher than the native carrier concentration. Moreover, the numbers of photon-generated electrons and holes are equal, so equation (12) can be rewritten

$$\Delta n\left(\Delta N,E\right) = \frac{hc}{\pi e}\int_0^\infty \frac{\Delta\alpha\left(\Delta N,E'\right)}{E'^2-E^2}{\rm d}E'. \quad (13)$$

The refractive index changes of the TE mode and TM mode are given by

$$\Delta n_{\rm TE}\left(\Delta N,E\right) = \frac{hc}{\pi e}\int_0^\infty \frac{\Delta\alpha_{\rm TE}\left(\Delta N,E'\right)}{E'^2-E^2}{\rm d}E', \quad (14)$$

$$\Delta n_{\rm TM}\left(\Delta N,E\right) = \frac{hc}{\pi e}\int_0^\infty \frac{\Delta\alpha_{\rm TM}\left(\Delta N,E'\right)}{E'^2-E^2}{\rm d}E'. \quad (15)$$

So far, we have deduced the relationship between the refractive index changes of TE and TM and the photon-generated carrier concentration. We have obtained a theoretical model of the refractive index changes of TE and TM.

3. Simulation analysis

Based on the above theory, the influence of light intensity and photon-generated carrier concentration on the refractive index difference between the TE and TM modes is analyzed. In order to determine the material of EAM, the signal light and pump light are chosen. Light at 1310 nm and 1550 nm is used in the field of communication. Because the variation of refractive index caused by the change of carrier concentration is relatively significant in the long-wave band, light sources at 1550 nm and 1310 nm are chosen as the signal and pump lights. The material selected for the EAM is $In_{0.53}Ga_{0.47}As$, due to its strong absorption of pump light. For this material, the refractive index is 3.67, the quantum efficiency is almost 1, and the reflection coefficient is 30%. For $E_{\rm g} = 0.798$ eV, $m_{\rm e} = 0.041m_0$, $m_{\rm hh} = 0.45m_0$, and $m_{\rm lh} = 0.052m_0$,[15] the recombination efficiency $B_{\rm r}$ is estimated to be $B_{\rm r} = 2.5\times10^{-21}$ m^3/s.[16]

A simulation is carried out to analyze the refractive index difference between the TE and TM modes. Figure 2 shows the changes of photon-generated carrier concentration along z

under different intensities of pump light. The pump light is stronger and has a greater carrier concentration. The rate of carrier concentration decay depends on the EAM absorption coefficient, and it declines rapidly when the pump light intensity is greater.

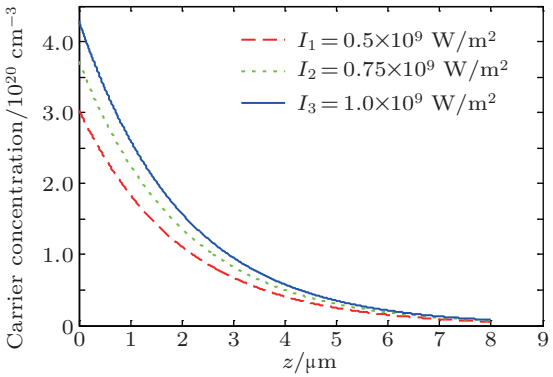


Fig. 2. (color online) Photon-generated carrier concentration in the longitudinal direction.

An increase of carrier concentration increases the probabilities that electrons and holes occupy the conduction band and valence band respectively. From Eqs. (10) and (11), we can see that these probabilities impact the absorption coefficients. So a change of carrier concentration will affect the absorption coefficients for the signal light. In accordance with Eqs. (10) and (11), when the photon-generated carrier concentration is two orders of magnitude more than the original carrier concentration, the absorption coefficients of TE and TM will significantly change along with the light wavelength. As shown in Fig. 3, when the carrier concentration is 10^{20} cm^{-3}, the decreased values of the TE and TM modes' absorption coefficients is not the same under the same photon-generated carrier concentration. The absorption of the TE mode is less than that of the TM mode, while the input light wavelength is near the band gap.

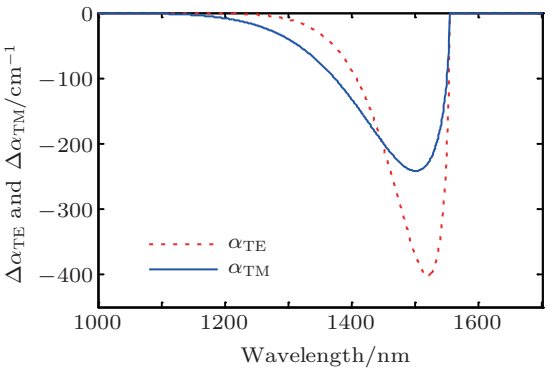


Fig. 3. (color online) Changes of TE and TM absorption coefficients as functions of wavelength.

According to Eqs. (14) and (15), for a certain photon-generated carrier concentration, the changes of the TE and TM refractive indices as functions of input light wavelength are presented in Fig. 4. The break point near 1550 nm corresponds to the band gap wavelength. Light with photon energy less than the band gap energy cannot be absorbed.

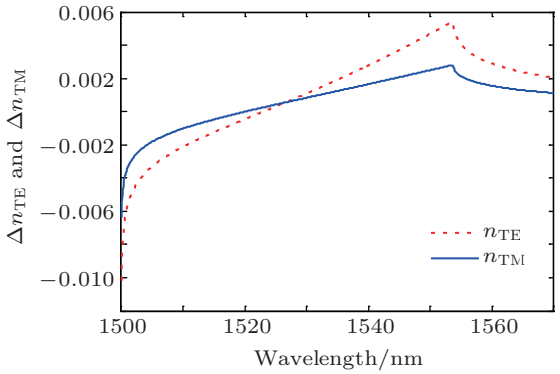


Fig. 4. (color online) Changes of TE and TM refractive indices as functions of wavelength.

The relationships between the absorption coefficients of the TE and TM modes and the photon-generated carrier concentrations are shown in Fig. 5. The absorption of the TM mode is greater than that of the TE mode near 1550 nm. As the photon-generated carrier concentration grows, the difference of the absorption coefficients increases.

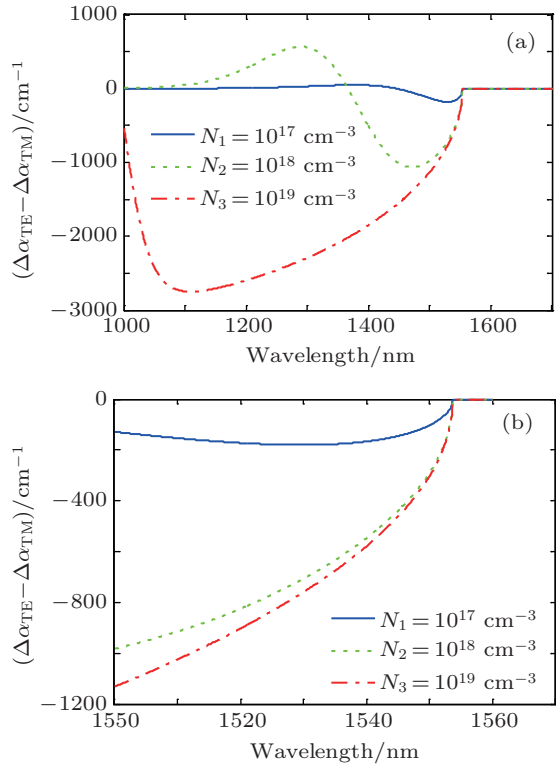


Fig. 5. (color online) The change of α_{TE}–α_{TM} as a function of wavelength (a) in a wide range of wavelengths and (b) near the band gap wavelength.

From Eqs. (14) and (15), we can plot the refractive index difference between the TE and TM modes. The n_{TE}–n_{TM} value is greatest when the signal wavelength is close to the band gap wavelength. Moreover, the greater the carrier concentration,

the higher n_{TE}–n_{TM}. But when the carrier concentration is greater than 10^{18} cm^{-3}, the value of n_{TE}–n_{TM} does not change much.

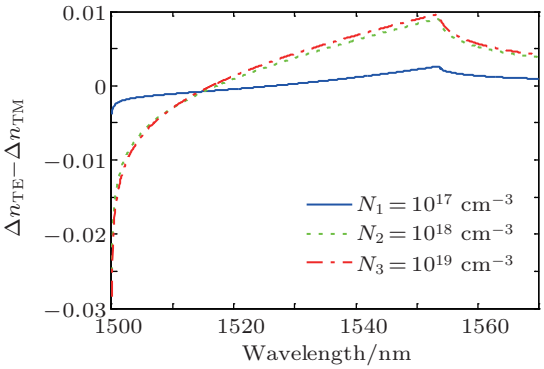


Fig. 6. (color online) The change of n_{TE}–n_{TM} as a function of wavelength.

Above all, the refractive index difference between the TE and TM modes in the EAM has been demonstrated. The difference can lead to rotation of the polarization of the signal light. Hence, a novel all-optical fiber loop buffer based on the polarization rotation effect in the EAM can be designed.

4. Design of all-optical buffer

The schematic diagram of all-optical fiber loop buffer is given in Fig. 7. The continuous lights at 1310 nm and 1550 nm are chosen as the pump and signal. The signal light goes into the EAM through a coupler and a wavelength division multiplexer (WDM), while the pump light is coupled to the EAM through WDM. The orientation of the signal light's polarization with respect to the EAM waveguide surface is 45°. Since the photon-generated carrier concentration is determined mainly by the pump light, the output of the signal light is kept constant directly through the "1" port of the polarization beam splitter (PBS) when there is no pump light. With the pump light is on, the refractive indices of the TE and TM modes each change differently. The refractive index difference has a determined effect on the phase difference between the TE and TM modes. When the phase difference reaches π, the polarization of the output signal light will rotate 90°. Then the output signal light passes through the "2" port of PBS to the fiber loop. In the fiber loop, there is a band pass filter (BPF) of 1550 nm to get rid of the 1310-nm wavelength and an EDFA that amplifies the signal light. A PC3 makes sure the polarization direction of the signal light with respect to the EAM waveguide surface is 45°, so the signal light circles in the fiber loop. The absorption of the signal light can be ignored because of the EAM saturated absorption effect under the strong pump light. The buffer can read out signals while there is no pump light in EAM.

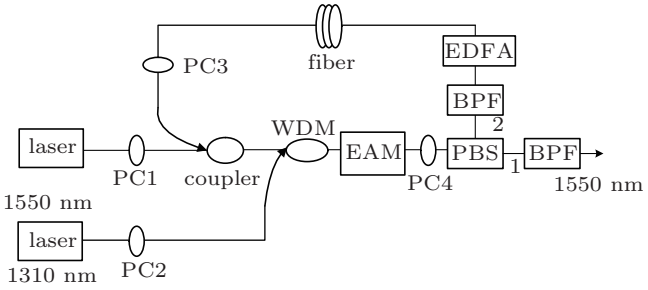


Fig. 7. Schematic diagram of the buffer.

When the signal light is emitted out of the EAM, the phase difference between the TE and TM modes is

$$\Delta\varphi = (n_{\mathrm{TE}} - n_{\mathrm{TM}}) \cdot d \cdot \frac{2\pi}{\lambda}, \tag{16}$$

where d is the length of the effect region and λ is the wavelength of the signal light. We chose pump light intensity $I_0 = 10^9$ W/m^2, $d = 100$ μm, and $\lambda = 1550$ nm. Combining these values with Eqs. (14) and (15), the relationship between the phase difference and the signal light wavelength can be obtained, as shown in Fig.8. The phase difference exceeds π near 1550 nm. When the intensity of the pump light equals 8.75×10^8 W/m^2, the phase difference equals π at 1550 nm.

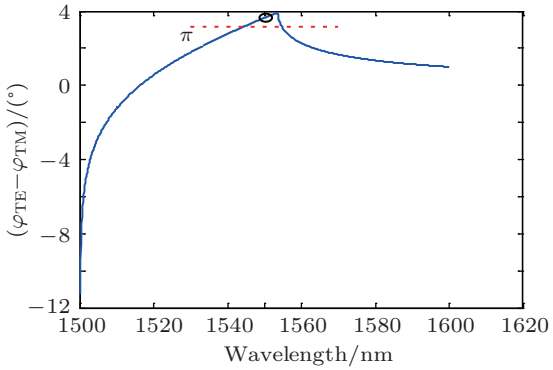


Fig. 8. (color online) Change of phase difference as a function of wavelength.

According to the above analysis, the polarization rotation effect can be achieved by injecting strong pump light into the EAM. Therefore, the novel all-optical fiber loop buffer design is feasible.

5. Conclusion

In summary, a theoretical model of the refractive index changes of the TE and TM modes along with photon-generated carrier concentration in the EAM was deduced. Then the variation of photon-generated carrier concentration and the absorption coefficient changes of the TE and TM modes for a given EAM were analyzed. According to the Kramers–Kronig constraints, the relationship between the refractive index changes of the TE and TM modes and wave-

length was presented. As the refractive index difference between the TE and TM modes reaches π, the polarization rotation effect was obtained. Using the polarization rotation in an EAM, a novel all-optical fiber loop buffer was designed.

References

[1] Liu A M, Wu C Q and Wang X Y 2001 *Photon Technology* **1** 204

[2] Zhang L J, Wu C Q and Li Y J 2007 *Acta Opt. Sin.* **27** 1945

[3] Li Y M, Hu W X, Cheng B W, Liu Z and Wang Q M 2012 *Chin. Phys. Lett.* **29** 034205

[4] Jia L M and Chen G X 2007 *Opt. Commun. Technol.* **31** 41

[5] Ji Y, Li Y, Wu J, Zhang F Z, Xu K, Li W, Hong X B and Lin J T 2012 *IEEE Photon. Technol. Lett.* **24** 64

[6] Liao Z Y, Yang H and Wang W 2008 *Chin. Phys. B* **17** 2557

[7] Wang Y, Pan J Q, Zhao L J, Zhu H L and Wang W 2010 *Chin. Phys. B* **19** 124215

[8] Zhang Y X, Liao Z Y, Zhao L J, Pan J Q, Zhu H L and Wang W 2010 *Chin. Phys. B* **19** 074216

[9] Bouchaib H, Zhang X P, Jiang W, Wu K, Liu T J, Xu T F, Nie Q H and Xu K 2011 *IEEE Photon. Technol. Lett.* **23** 230

[10] Li H F 2009 *Opto-Electronic Engineering* **36** 85

[11] Huo L, Yang Y F, Nan Y B, Lou C Y and Gao Y Z 2006 *Lightwave Technology* **24** 3035

[12] Liu E K, Zhu P S and Luo J S 2011 *Semiconductor Physics*, 7th edn. (Beijing: National Defense Industry Press) p. 254

[13] Brian R B, Richard A S and Jesus A D A 1990 *Quantum Electronics* **26** 113

[14] Chen K J, Yang A L and Jiang X Q 2002 *Opt. Instrum.* **24** 86

[15] Zhou S L, Chong Y Z, Huang Y Q and Ren X M 2005 *Semicond. Technol.* **30** 20

[16] Brain R B and Richard A S 1987 *Quantum Electron* **23** 2159